# $H^-$ and $D^-$ production by backscattering from alkali-metal targets

P. J. Schneider,* K. H. Berkner, W. G. Graham, R. V. Pyle, and J. W. Stearns
*Lawrence Berkeley Laboratory, University of California, Berkeley, California 94720*
(Received 14 July 1980)

Measurements have been made of the total backscattered $D^-$ and $H^-$ yields from thick, clean targets of Cs, Rb, K, Na, and Li, bombarded with $H_2^+$, $H_3^+$, $D_2^+$, $D_3^+$ with incident energies from 0.15 to 4.0 keV/nucleus. All of the measurements were made at background pressures less than $10^{-9}$ Torr, and the alkali-metal targets were evaporated onto a cold substrate ($T \sim 77$ K) *in situ* to assure thick, uncontaminated targets. For each target, the $H^-$ and $D^-$ yields exhibited maxima (as high as 0.08 per incident proton and deuteron) at incident energies between 0.3 and 1.4 keV/nucleus. For both hydrogen and deuterium incident at any energy, the negative-ion yield decreases in going from Cs to Li in the order given above. Also, a definite isotope effect was observed for every target used, with the $H^-$ yield peaking at a lower incident energy than the $D^-$ yield and in most cases, the maximum $H^-$ yield was higher than the maximum $D^-$ yield. Measurements of the $D^-$ yield as a function of Cs coverage were also made for $D_3^+$ bombarding a Ni substrate. The $D^-$ yield maximized at or near the coverage at which the surface work function reached a minimum.

## I. INTRODUCTION

Recent experiments have shown that it is possible to dramatically increase negative-ion yields from ion sources by adding an alkali metal to the discharge.[1,2] In $H^-$ sources, the addition of Cs to the discharge has resulted in increases of more than an order of magnitude in the $H^-$ current density.[3] Belchenko, Dimov, and Dudnikov[3–5] and Hiskes, Karo, and Gardner[6] have proposed models based upon surface production as the principal mechanism for $H^-$ formation in these sources. Belchenko, Dimov, and Dudnikov proposed that any hydrogen atom adsorbed on the surface has a high probability of residing as a negative ion and can be desorbed from the surface as a negative ion by an incident energetic particle from the discharge. The addition of Cs to the $H^-$ source produces Cs coverage of the source surfaces; this lowers the surface work function, enhances the probability of escape without destruction of the negative ion from the surface, and increases the $H^-$ yield. Hiskes, Karo, and Gardner have hypothesized that $H^-$ ions are formed in the collision of an energetic (1 to 100 eV) hydrogen atom with an adsorbed Cs atom. The $H^-$ formation process takes place via the CsH, $CsH^-$ molecular potentials: As the hydrogen atom approaches the adsorbed Cs atom the interaction potential is taken to be the difference between the image potential and the $CsH^-$ electron affinity. This potential allows the resonant transfer of an electron from the substrate to the hydrogen atom, which in turn may escape from the surface as $H^-$.

$H^-$ production from surfaces involves three processes: The reflection or desorption of the hydrogen from the surface, the formation of the negative ion at the surface, and the escape without destruction of the negative ion from the surface. In the mechanism proposed by Belchenko, Dimov, and Dudnikov,[3–5] the probability of formation of the negative ion is unity and the probabilities of desorption and escape without destruction become the dominant factors in determining the negative-ion yield from the surface. In the partial-coverage model of Hiskes and Karo,[7] the probability of destruction of the negative ion is shown to be negligible, so that the probability of formation of the negative ion, along with the probability of reflection of the incident particle, become the dominant factors in determining the negative-ion yield from the surface.

These models have led to calculations of the $H^-$ secondary emission coefficient (the number of negative ions emitted from the surface per incident nucleus) by Kishinevskii[8] and Hiskes and Karo.[7] Kishinevskii has estimated the $H^-$ secondary emission coefficient to be 0.1 to 0.2 for particles leaving the surface with energies of tens of eV. Hiskes and Karo have calculated both formation and escape probabilities for surfaces with a partial monolayer coverage of Cs. They have combined their results with those of Oen and Robinson,[9] who have used a Monte Carlo technique to calculate the reflected fraction of the incident particles as a function of incident energy, to predict $H^-$ secondary emission coefficients of 0.5 to 0.3 over the backscattered-energy range 10 to 100 eV. Hiskes and Karo[7] have also calculated the escape probabilities from some thick alkali-metal surfaces.

There exist almost no experimental measurements for comparison with the above calculations. Therefore, we have measured the total backscattered $H^-$ and $D^-$ yields from various alkali-metal surfaces. The experiment was dividied into two parts: (1) clean, thick, alkali-metal tartets (Cs, Rb, K, Na, and Li) and (2) thin coverage of Cs on an Ni substrate. For the thick targets, the incident energy of the hydrogen and deuterium ions ranged from 0.15 to 4 keV/nucleus and for the thin-coverage targets the range was from 0.4 to 0.9 keV/nucleus.

For reasons discussed in the next section it was necessary to use molecular ions: $D_2^+$, $D_3^+$, $H_2^+$, and $H_3^+$. At the energies used here, molecular ions at normal incidence are dissociated at the surface,[10,11] hence the $D^-$ and $H^-$ yields were normalized to the number of nuclei per incident ion to obtain $D^-$ per incident deuteron or $H^-$ per incident proton. The $D_3^+$ and $H_3^+$ ions were used to obtain the lowest incident velocities, due to the limit imposed by low-energy beam transport to the target. The $D_2^+$ and $H_2^+$ ions were used to verify that the negative-ion yields were indeed independent of the number of nuclei per incident molecular ion.

By varying the energy of the incident ions, the work function and the mass of the target, we have attempted to determine which parameters are important to the conversion of incident particles to backscattered negative ions and how these parameters may be varied to optimize the negative-ion yield.

## II. APPARATUS AND PROCEDURE

A beam of $D_2^+$ ($H_2^+$) and $D_3^+$ ($H_3^+$) ions was extracted from a hot-filament discharge, accelerated to the desired energy, and momentum selected with a 30° bending magnet before entering the experimental chamber, which is described in greater detail in Ref. 12. The apparatus within the chamber (Fig. 1) was designed around two rectangular plates, perpendicular to the beam line; an aperture in the first plate (the collector) allowed the beam to pass through to the second plate (the target) from which $D^-$ ($H^-$), $D^0$ ($H^0$), $D^+$ ($H^+$), $e^-$ as well as sputtered particles were emitted. The collector was used to monitor the negative-ion current, therefore, all other charged particles had to be prevented from reaching or leaving it: An electric field between the target and collector plates prevented positive secondary ions from reaching the collector and a transverse magnetic field suppressed secondary electrons. Also, an upbeam collimator shielded the collector from the primary beam. This collimator was the endplate of a Faraday cup (the collimator-Faraday cup) which was used to determine the total current incident onto the target: The total incident current was determined by the difference in current readings from the collimator-Faraday cup when the beam was deflected into the cup and when it was steered through the cup by a pair of upbeam deflection plates. The negative-ion secondary-emission coefficient (NISEC) was determined by taking the ratio of the collector current to the total incident current and dividing by the number of deuterons (protons) per incident molecular ion.

The collimator-Faraday cup, which was 2.5 cm in diameter, 4 cm long and had a 0.15-cm-diam exit aperture, was 0.08 cm upbeam from the collector.

The electric field used to suppress positive ions was produced by applying a negative voltage to the target. The magnitude of the applied voltage was determined by the beam species and energy. As an example, a 5.0-keV beam of $D_3^+$ required a target bias of at least $-2.5$ kV. The target bias adds to the incident energy giving a total incident energy of 7.5 keV; if we assume that the energy is divided equally between the three deuterons as the incident ion breaks up at the surface, then the maximum energy that a reflected $D^+$ ion can have is less than 2.5 keV, which is not sufficient for it to reach the collector plate. This explains why, in this experiment, $D^+$ and $H^+$ were not used as incident particles. For $D^+$ the maximum reflected energy is always greater than the retarding voltage, so that the high-energy backscattered $D^+$ ions cannot be prevented from reaching the collector.

The transverse magnetic field used to suppress secondary electrons from the target, the collector and the collimator-Faraday cup was produced by an electromagnet with a 6.5-cm gap and 5-cm-diam poles. The suppression of secondary electrons is illustrated in Fig. 2, where the "apparent" NISEC is plotted versus the magnitude of the magnetic field. At low magnetic fields the signal is dominated by electrons, which are suppressed as the magnetic field is increased. For the case illustrated in Fig. 2

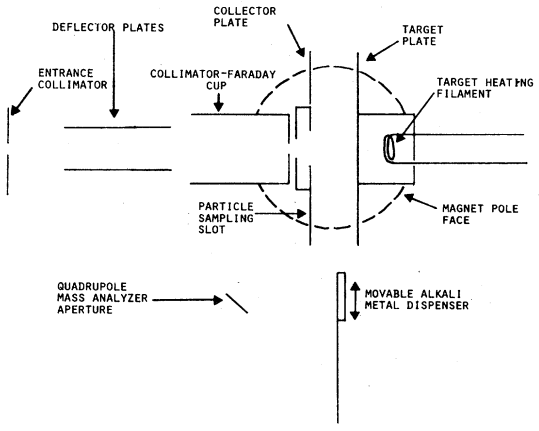


FIG. 1. Line drawing of the apparatus within the experimental chamber, which was used to measure the negative-ion secondary-emission coefficient (NISEC).

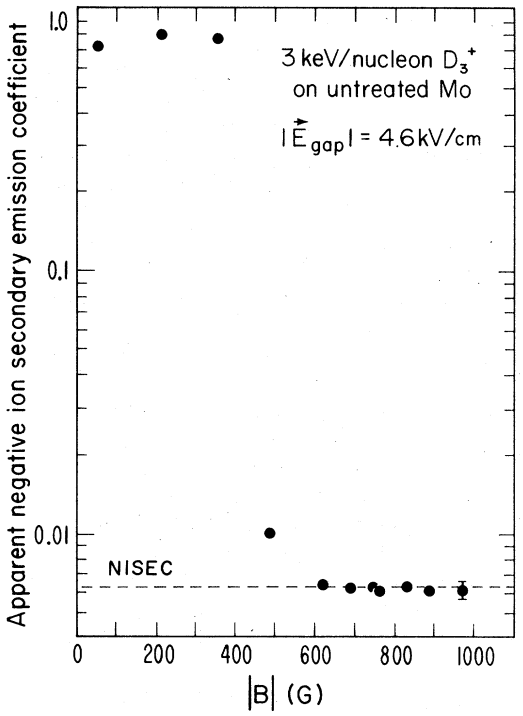


FIG. 2. Apparent NISEC vs the magnitude of the applied magnetic field for the case of 6 keV/deut. $D_3^+$ on an untreated Mo target. The target bias was −6 kV, resulting in an electric field of 4.6 kV/cm.

(3 keV/nucleon $D_3^+$, $|E_{gap}| = 4.6$ kV/cm) 650 G is sufficient for complete electron suppression. Calculations of trajectories for $D^-$ ions emitted from the target show that all negative ions (even those emitted with zero energy) reach the collector for all electric and magnetic fields used in this experiment.

The target and collector plates were 7.3 cm high, 5 cm wide, and separated by 1.3 cm; the collector-plate aperture was 0.25 cm in diameter. To assure that all the negative ions produced at the target were collected, two separate tests were performed. The first test was to vary the effective width of the collector plate with a series of electrically isolated masks. The currents collected by the masks and by the collector were measured as a function of collector width. The ratio of the collector current to the sum of these currents remained constant at 0.99 for collector widths down to 3.6 cm and decreased as the collector width was further decreased. The second test was to vary the effective diameter of the aperture in the collector plate from 0.25 to 0.7 cm with another series of electrically isolated masks which covered the collector plate. The ratio of the current on the mask to the current on the collector behind it was measured as a function of the diameter of the aperture. Extrapolation to zero diameter indicated that the loss of negative ions through the 0.25-cm-diam aperture was (5 ± 5)%. From these tests, which were performed for incident energies from 0.75 to 3 keV/nucleon and with various electric and magnetic fields, we concluded that the dimensions of the collector plate were large enough, and the aperture small enough, to ensure that (95 ± 5)% of the negative ions were collected.

Positive ions produced by backscattered particles (atoms and negative ions) striking the collector could not be suppressed. The current due to these ions leaving the collector adds to the current from the collected negative ions and is a possible source of error. To investigate the magnitude of this effect, the NISEC was measured for a sodium target, with a stainless-steel collector. Then the target was heated to evaporate the sodium onto the collector. The dispenser was used to recoat the target with sodium and the NISEC measurement was repeated. Changing the collector surface from stainless steel to sodium changes the collector work function from 4 to 2.3 eV and greatly changes the charge distribution of the backscattered particles leaving the collector (very few positive ions leave the sodium surface). No difference was seen in the NISEC measurements using the two collector surfaces.

Meishnev and Verbeek[13] and Eckstein *et al.*[14] have measured the ratio of protons to neutrals emerging from various metal targets as a function of exit energy and angle. Their results indicate that for an exit energy of 1 keV, less than 5% of the emerging particles are positive ions, with the positive-ion fraction dropping off rapidly at lower energies. These results, along with the measurements using the two collector surfaces, led to the conclusion that the effect of positive ions leaving the collector was less than the differences in reproducibility of the experimental measurements (5%).

Clean alkali-metal targets were deposited on a liquid-nitrogen-cooled substrate in the cryopumped experimental chamber, which was maintained at a pressure less than $10^{-9}$ Torr during the measurements. An SAES (SAES Getters/USA, Crystal Springs, Colorado) alkali-metal dispenser, mounted on a bellows, could be positioned between the target and collector plates to coat the target area. The thickness of the alkali-metal layer was controlled by varying the current through the dispenser (6 to 8 A) and the evaporation time. As an example, from the manufacturer's data we estimate that passing 7.5 A through an Na dispenser for 3 min results in an Na layer about 15 $\mu$m thick (assuming an Na sticking coefficient of unity), which is the same order of magnitude as the average penetration depth of a 1-keV deuteron.[15]

Surface purity was monitored by mass analysis of positive ions sputtered from the surface by an 8-keV

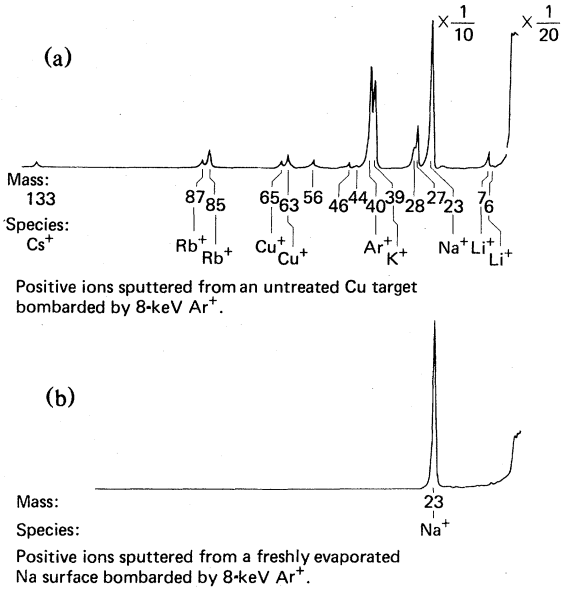


FIG. 3. Mass spectra of positive ions sputtered by 8-keV $Ar^+$ incident upon (a) an untreated Cu target and (b) the same Cu target with thick Na coverage.

$Ar^+$ beam. An electrostatic-quadrupole mass analyzer, was placed in the chamber so that it sampled ions leaving the surface at an angle of 50° to the surface normal.[12] Prior to evaporation, many different mass peaks were observed, indicating extensive surface contamination [Fig. 3(a)]; after a thick alkali-metal target was deposited, the positive-ion spectrum showed only peaks corresponding to sputtered alkali-metal target ions [Fig. 3(b)]. To determine if the sputtered impurity ions contributed significantly to the total negative-ion signal, incident beams of $Ar^+$ at 8 keV were used. The results showed that the *sputtered* negative ions (either $H^-$ or impurities) contributed less than 5% of the total negative signal on the collector; hence within our experimental estimated uncertainty of 10%, the NISEC measured in this experiment is the *backscattered* $H^-$ yield.

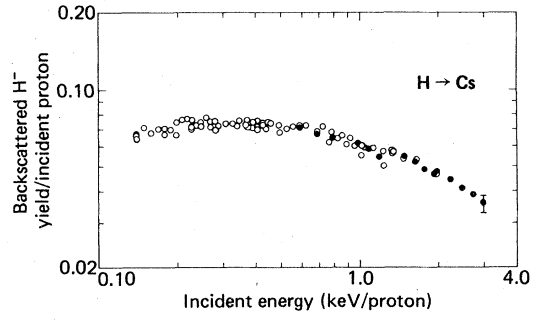


FIG. 4. Backscattered $H^-$ yield vs incident energy for $H_2^+$–(●) and $H_3^+$–(○) incident on thick Cs (work function, $\phi_w = 1.9$ eV).

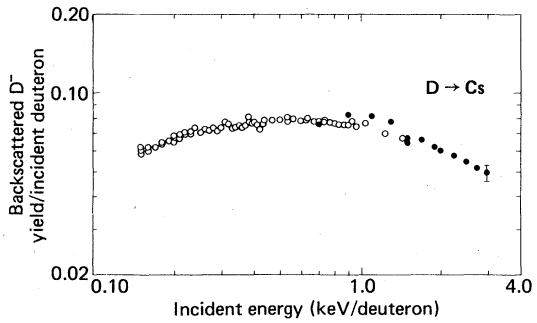


FIG. 5. Backscattered $D^-$ yield vs incident energy for $D_2^+$–(●) and $D_3^+$–(○) incident on thick Cs (work function, Cs $\phi_w = 1.9$ eV).

For $H^-$ yield measurements from thin coverage of a substrate, changes in the surface work function were measured using the retarding potential method.[15–18] A hot tungsten filament could be positioned directly in front of the target, and by measuring the shift in the *I-V* curves of the diode formed by the filament and the target, the change in the target work function relative to that of the filament was obtained.[12]

## III. RESULTS AND DISCUSSION

### A. Thick coverage

Figures 4 to 13 show the measured values of the backscattered $D^-$ and $H^-$ yields for Cs, Rb, K, Na, and Li targets as a function of the energy of the incident ions. The estimated standard uncertainties (±10%) indicated in the figures are the result of considering the effects discussed in the text (losses

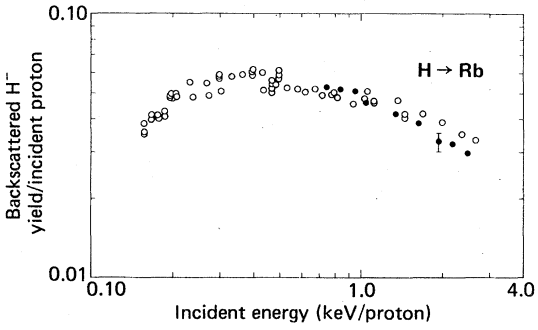


FIG. 6. Backscattered $H^-$ yield vs incident energy for $H_2^+$–(●) and $H_3^+$–(○) incident on thick Rb ($\phi_w = 2.08$ eV).

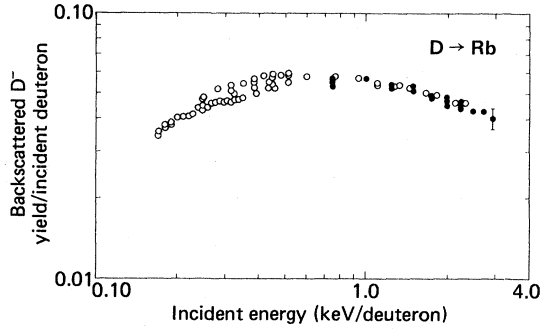


FIG. 7. Backscattered $D^-$ yield vs incident energy for $D_2^+$–(●) and $D_3^+$–(○) incident on thick Rb ($\phi_w = 2.08$ eV).

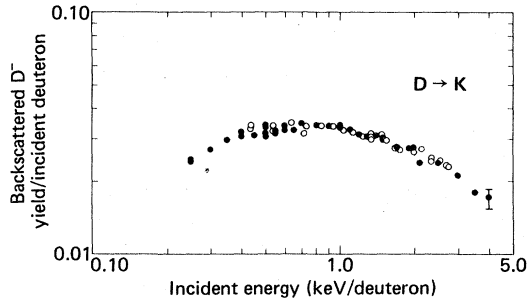


FIG. 9. Backscattered $D^-$ yield vs incident energy for $D_2^+$–(●) and $D_3^+$–(○) incident on thick K ($\phi_w = 2.24$ eV).

through the collector aperture and positive ions leaving the collector) as well as the calibration of the electrometers and reproducibility of the measurements.

There are some features worth noting in Figs. 4 through 13.

(1) Each target shows a maximum in the $H^-$ and $D^-$ yields.

(2) The maximum value of the $H^-$ ($D^-$) yield decreases in the order Cs, Rb, K, Na, and Li at any incident energy.

(3) The higher the maximum value of the $H^-$ ($D^-$) yield, the lower the incident energy at which it occurs.

(4) For any given target the maximum in the $D^-$ yield is less than or equal to the maximum in the $H^-$ yield and occurs at a higher incident energy than the $H^-$ maximum.

(5) The $H^-$ yield per incident proton is the same for $H_2^+$ and $H_3^+$ ions incident, and the $D^-$ yield per incident deuteron is the same for $D_2^+$ and $D_3^+$ incident, but, at a given incident energy, the $D^-$ and $H^-$ yields are not equal.

The results of these measurements can be interpreted by considering the $H^-$ yield as a function of the probability of reflection of the incident particles, $n(\bar{v})/N_i$, the probability of formation of the $H^-$ ion at the target $P_-(\bar{v})$, and the probability of the survival of the $H^-$ ion as it leaves the target $f(\bar{v})$. The $H^-$ yield ($Y$) is then given by

$$Y = \frac{1}{N_i} \int_v n(\bar{v}) P_-(\bar{v}) f(\bar{v}) d\bar{v} \quad . \tag{1}$$

If, for the sake of discussion, we assume that the terms are separable

$$Y = R_N f P_- \quad , \tag{2}$$

where, $R_N$ is the total particle reflection coefficient, $f$ is the (averaged) probability of $H^-$ survival, and $P_-$ is the (averaged) probability of $H^-$ formation.

To discuss the $H^-$ yield measurements in terms of Eq. (2), we need to know the dependence of $R_N$, $f$, $P_-$ on the incident energy. Hiskes has shown that calculated values of $R_N$ for alkali metals are a monotonically decreasing function of the incident energy, in the energy range of these measurements.[19]

In the accompanying paper,[20] Hiskes and Schneider show that $P_-$ is a monotonically decreasing function of the average perpendicular exit velocity, $\langle v_\perp \rangle$, which increases with increasing incident velocity. Similarly, $f$ is a monotonically increasing function of the incident velocity. Therefore, the fact that all the $H^-$ and $D^-$ curves have maxima at incident energies above 200 eV indicates that the survival probability is the major factor in determining the negative-ion yield at incident energies below a few hundred

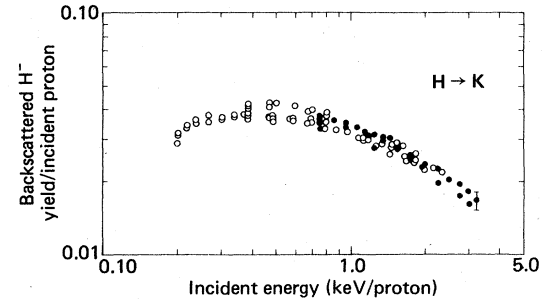


FIG. 8. Backscattered $H^-$ yield vs incident energy for $H_2^+$–(●) and $H_3^+$–(○) incident on thick K ($\phi_w = 2.24$ eV).

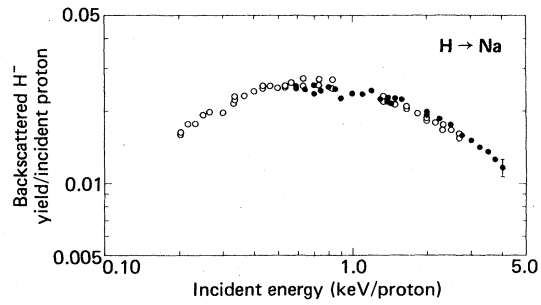


FIG. 10. Backscattered $H^-$ yield vs incident energy for $H_2^+$–(●) and $H_3^+$–(○) incident on thick Na ($\phi_w = 2.28$ eV).

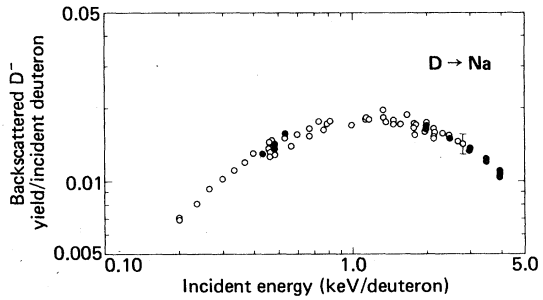


FIG. 11. Backscattered $D^-$ yield vs incident energy for $D_2^+$–(●) and $D_3^+$–(○) incident on thick Na ($\phi_w = 2.28$ eV).

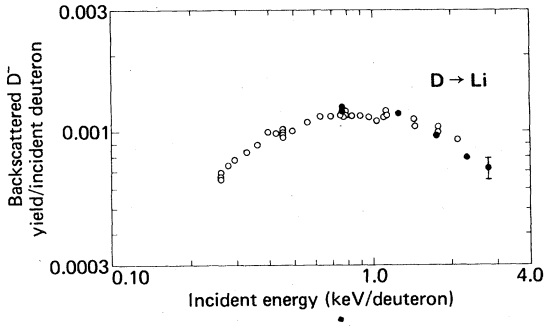


FIG. 13. Backscattered $D^-$ yield vs incident energy for $D_2^+$–(●) and $D_3^+$–(○) incident on thick Li ($\phi_w = 2.49$).

electron volts. Similarly, at high incident energies, the probability of formation and reflection are the factors determining the $H^-$, $D^-$ yields. Features (2) and (3) above, can be explained by the fact that at the same incident energy the reflection probability decreases in the order given in feature (2) and that the work function increases in the same order: The lower the work function, the larger the survival probability at lower incident energies, thus shifting the $H^-$, $D^-$ yield maximum to lower incident energy.

The isotope effect [features (4) and (5)] arises from the fact that $R_N$, $f$, and $P_-$ have different energy dependences. $R_N$ is almost the same for H and D at the same incident energy. However, the incident velocity and the average reflected velocity are higher for H than for D. Thus, at low incident energies, where survival probability dominates, $H^-$ has a higher survival probability and hence a higher yield than $D^-$. On the other hand, at high incident energies, where formation probability dominates, $D^-$ has a higher formation probability, and thus a higher yield than $H^-$. This argument also explains the crossing over of the $H^-$ and $D^-$ yield curves. The fact that the isotope effect becomes more pronounced as the target mass and atomic number become smaller is probably due to the mass difference between H and D (1 amu) becoming more significant compared to the target mass (133 amu for Cs to 7 amu for Li), thus giving rise to different velocity distributions of $H^-$ and $D^-$ leaving the target.

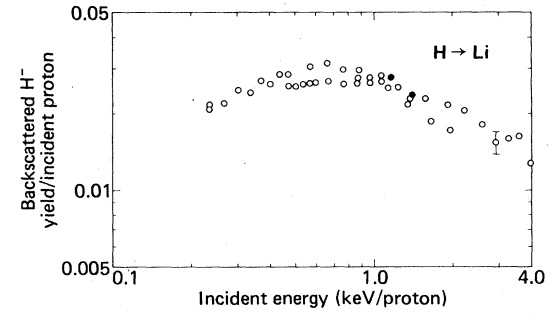


FIG. 12. Backscattered $H^-$ yield vs incident energy for $H_2^+$–(●) and $H_3^+$–(○) incident on thick Li ($\phi_w = 2.49$).

### B. Thin coverage

The thin-coverage measurements were made using cesium on an Ni substrate. This combination of materials was chosen because of the low value of the minimum work function (1.6 eV)[21] which can be obtained at a fractional Cs monolayer coverage of the Ni surface, and because Ni was a convenient material to work with. In Fig. 14, we show the change in the surface work function and the backscattered $D^-$ yield as the Cs coverage is increased on a Ni substrate which was cleaned by abrasion before being installed in the vacuum chamber. The substrate was heated to about 1400 K, hot enough to deposit a clearly visible Ni layer on the facing collector plate in about 30 min, at a background pressure of $10^{-9}$ Torr, and was allowed to cool to room temperature overnight at a background pressure of $4 \times 10^{-10}$ Torr before the Cs was evaporated. It can be seen in Fig. 14 that the maximum in the backscattered $D^-$ yield occurs at the Cs coverage that produces the minimum work function, for both 170- and 550-eV/deut. incident energies. The maximum $D^-$ yield of 0.14 for thin coverage is almost twice as high as the maximum of 0.08 for thick Cs (see Fig. 5). The variation of the backscattered $D^-$ yield with incident energy, as the Cs coverage is increased on a Ni substrate, is illustrated in Fig. 15. The backscattered $D^-$ yield curves show a definite change in energy dependence as the Cs coverage is increased: At low Cs coverages the $D^-$ yield decreases as the energy decreases, at optimum Cs coverage (evaporation No. 9) the $D^-$ yield increases with decreasing energy, and at thicker coverage (evaporation No. 11) the $D^-$ yield again decreases with decreasing energy. This change in the energy dependence may be explained by a hypothesis presented by Hiskes and Karo[7] for $D^-$ yields from $W$ with a partial monolayer of Cs coverage: At partial monolayer

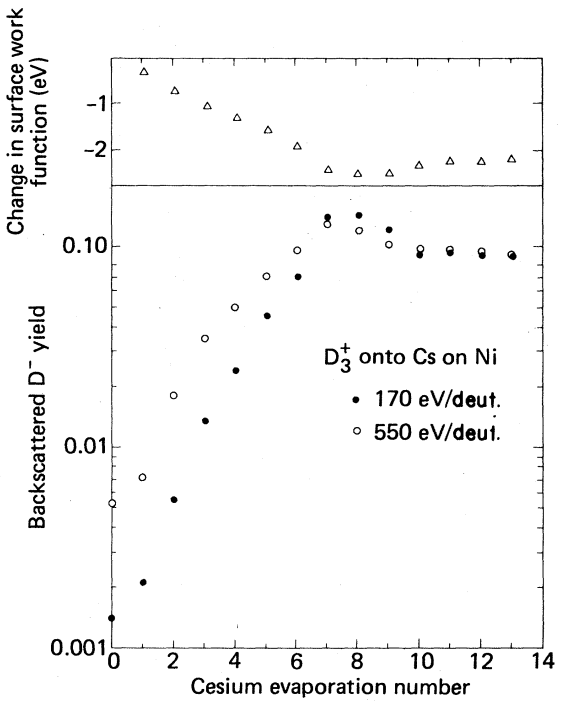


FIG. 14. Backscattered $D^-$ yield and change in surface work function vs evaporation number for Cs deposited on a room-temperature Ni substrate: Δ, change in work function; ●, 170-eV/deut. $D_3^+$ incident; ○, 550-eV/deut. $D_3^+$ incident.

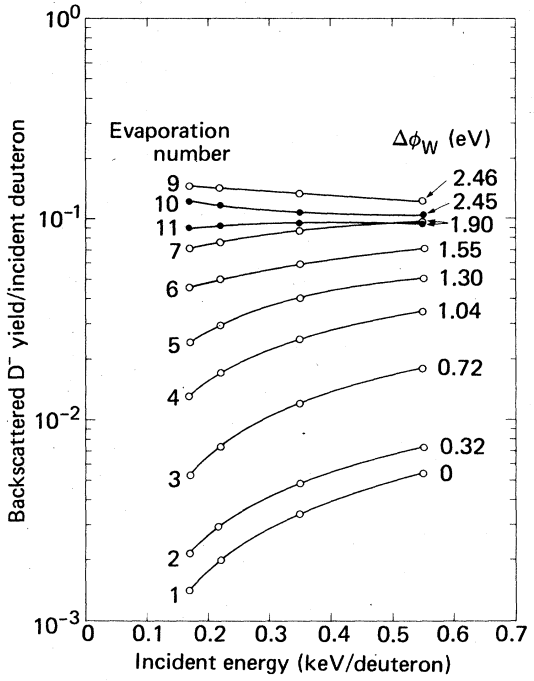


FIG. 15. Variation of the backscattered $D^-$ yield with incident energy as the Cs coverage is increased on a Ni substrate. The numbers to the right of the curves denote the change in the surface work function and those on the left indicate the evaporation number. The Cs thickness increases with evaporation number. The solid circles indicate Cs thickness beyond optimum coverage.

coverages, near the minimum in the work function, an electric dipole layer is produced at the Cs-substrate interface, which greatly enhances the probability of survival of the $D^-$. As discussed in the preceding section, the probability of survival dominates the backscattered $D^-$ yield for incident energies below a few hundred eV, so that any change in the survival probability should be apparent in the $D^-$ yield. For higher incident energies, the $D^-$ yield depends more upon the probability of formation than survival, so that the effect of the dipole layer will not be as pronounced.

A quantitative discussion of these results is presented in the accompanying paper by Hiskes and Schneider.[20]

## ACKNOWLEDGMENTS

We gratefully acknowledge H. A. Hughes, L. A. Biagi, and the members of their mechanical shops and also C. M. Garrett for maintenance of the electronics associated with the experiment. Work was supported by the U.S. Department of Energy, Office of Fusion Energy under Contract No. W-7405-ENG-48.

*Present address: Max Planck Institute for Plasmaphysics, Garching, West Germany.

[1]K. W. Ellers and K. N. Leung, Rev. Sci. Instrum. 51, 721 (1980).
[2]R. Middleton, IEEE Trans. Nucl. Sci. 23, 1098 (1976).
[3]Yu. I. Belchenko, G. I. Dimov, and V. G. Dudnikov, Izv. Akad. Nauk SSSR Ser. Fiz. 37, 2573 (1973).
[4]Yu. I. Belchenko, G. I. Dimov, and V. G. Dudnikov, Zh. Tekh. Fiz. 45, 68 (1973) [Sov. Phys. Tech. Phys. 20, 40 (1975)].
[5]G. I. Dimov, presented at the Second Symposium on Ion Sources and Formation of Ion Beams, Berkeley, California, 1974 [LBL Report No. 3399 Suppl. (unpublished)].
[6]J. R. Hiskes, A. Karo, and M. Gardner, J. Appl. Phys. 47, 3888 (1976).
[7]J. R. Hiskes and A. Karo, LBL Report No. 6839 (1977) (unpublished).
[8]M. E. Kishinevskii, Report No. IYAF 76-18 (1976) (unpublished).
[9]O. S. Oen and M. T. Robinson, Nucl. Instrum. Methods 132, 647 (1976).

[10]W. Eckstein, H. Verbeek, and S. Datz, Appl. Phys. Lett. 27, 527 and 528 (1975).
[11]A. Heiland, U. Beitat, and E. Taglauer, Phys. Rev. B 19, 1677–1681 (1979).
[12]P. J. Schneider, Ph.D. thesis (University of California, Berkeley, 1980) (unpublished).
[13]P. Meischnder and H. Verbeek, Report No. IPP 9/18 (1975) (unpublished).
[14]W. Eckstein, P. Matschke, and H. Verbeek, in *Proceedings of the Second Conference on Surface Effects in Controlled Fusion Devices, San Francisco, California, 1976,* edited by W. Bauer, C. F. Finfgeld, and M. Kaminsky (North-Holland, Amsterdam, 1976), p. 199.
[15]J. R. Hiskes, private communication of results from the Marlowe Code (Ref. 9).
[16]P. A. Anderson, Phys. Rev. 47, 958 (1935).
[17]C. Herring and M. H. Nichols, Rev. Mod. Phys. 21, 185 (1949).
[18]J. Millman and S. Seely, *Electronics* (McGraw-Hill, New York, 1955), p. 107.
[19]J. R. Hiskes, J. Phys. (Paris) 40, C7-179 (1979).
[20]J. R. Hiskes and P. J. Schneider, Phys. Rev. B 23, 949 (1981) (following paper).
[21]C. A. Papageorgopoulos and J. M. Chen, Surf. Sci. 52, 40–52 (1975).